PRESSURE DROP OF FLOW THROUGH PERFORATED PLATE

José A. Barros Filho, jabf@cdtn.br
Moysés A. Navarro, navarro@cdtn.br
Brazilian Nuclear Energy Commission (CNEN/CDTN), Belo Horizonte, 30123-901, Minas Gerais, Brazil

Felipe A. P. Magalhães, fapmbr@yahoo.com.br
André A. Campagnole dos Santos, acampagnole@yahoo.com.br
Federal University of Minas Gerais, (UFMG/DEMEC), Belo Horizonte, 31270-901, Minas Gerais, Brazil

Abstract. The numeric modeling of flow through complex geometry has experienced a great progress within the last years. Therefore there is an increasing interest in the application of three dimensional computational fluid dynamics (CFD) codes in the field of nuclear technology. With further progress in safety analysis techniques, the increasing use of CFD codes for nuclear applications is expected. At present, the main objective with respect to CFD codes is generally to improve confidence in the available analysis tools and to achieve a more reliable approach to safety relevant issues. Aiming towards these goals, we present here the results of the first part of a research program devised to develop and validate a CFD methodology to simulate the flow of water through perforated plates with geometry similar to the ones of the bottom end piece of a Pressurized Water Reactor. This component drives the coolant into the core, promotes an adequate mixing of dissolved substances and holds the fuel assembly mechanically in place. It accounts for a great part of the pressure loss through the core. We present here the experimental pressure loss of water flow through 5 different perforated plates. The recovering pressure profile downstream of the plates was also measured. The experimental results were compared with numerical modeling performed with the commercial code CFX 10.0. Different mesh refinement and turbulence models were evaluated.

Keywords: pressure drop, perforated plate, CFD, turbulence models

1. INTRODUCTION

During design period and start up operation of a nuclear power plant (NPP) an exhaustive set of safety analysis simulations are required by national nuclear regulatory bodies for licensing purposes. In general, the simulations are carried out using vendor-specific design codes and best-estimate system analysis codes. These thermal-hydraulic system codes have powerful features such as multi-phase flow model, phase-change model and event programming. These codes, developed in the 70's, are not mechanistic, but based on one dimensional (1D) lumped parameter models. They do not solve the Navier-Stoke's equation but Euler equation, and so, the users are required to provide information about head loss, mixing rates or heat transfer in the form of empirical coefficients. The accuracy of these values is not guaranteed, however, because the structure of reactor vessel (RV) itself and its internals are very complicated. The correct values could be evaluated if full scale hydraulic experiments simulating real nuclear reactors were performed. But this is not practical. On the other hand, a plausible method to raise those coefficients is to calculate them using mechanistic computational fluid dynamics (CFD) codes. These codes solve the Navier-Stoke's equation, usually in its Reynolds averaged form, taking into account detailed geometric information of the flow. The treatments of turbulence, near wall velocity and heat transfer are performed by many different mathematical models available in the codes.

Computational fluid dynamics has undergone a great development in the last decade, mainly due to the enhancement of computing capacity. There is, therefore, an increasing interest in the application of CFD codes in the nuclear field, as it can be seen by the number of papers released in the related literature. They report the simulation of the flow in components of reactor vessels (Liu, 2005; Aszodi, 2002; Hoehne, 2000; Anglart, 1997) and even in complete sub-assemblies of the vessel (Jeong, 2005). With further progress in safety analysis techniques, the increasing use of CFD codes for nuclear applications is expected (Yadigaroglu, 2003; IAEA, 2001, 2002). Recently, the main objective with respect to CFD codes is generally to improve confidence in the mathematical models available through validation against experiments. Aiming towards these goals, a research program was devised in the Centro de Desenvolvimento da Tecnologia Nuclear-CDTN to develop and validate a CFD methodology to simulate the water flow through perforated plates with geometry similar to the ones of the bottom end piece of a Pressurized Water Reactor -PWR. The bottom end piece drives the coolant into the core, promotes an adequate mixing of dissolved substances and holds the fuel assembly mechanically in place. It accounts for a considerable amount of the pressure loss through the core. Figure 1 shows the bottom end of a typical PWR fuel assembly with the bottom end piece in detail.

This work presents the results of the first part of that program. The pressure losses of water flow through 5 perforated plates were measured. The recovering pressure profile downstream of the plates was measured as well. It also presents the numerical modeling of the tests, performed with the commercial CFD code, CFX 10.0 (CFX, 2006).
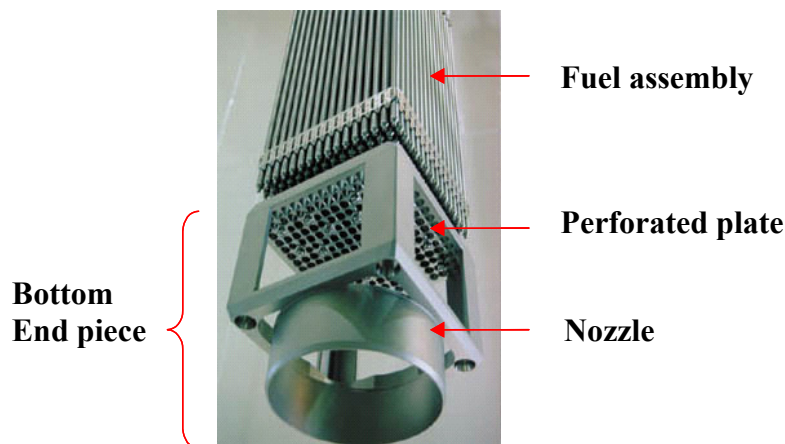
Figure 1. Fuel assembly with the bottom end piece.

Perforated plates have also been studied as flow conditioners for measuring stations (Schlüter and Merzkirch, 1996; Spearman et al, 1996), as distillation trays to increase the heat and mass transfer between fluids (Lockett, 1986) and as flow controller emerging from diffuser (Sahin and Ward-Smith, 1987).

The agreement between the pressure loss coefficients of perforated plates obtained from some experiments (Gan and Riffat, 1997) and that defined by Idelchik (1960) are not always acceptable.

Although the considerable amount of studies on numerical simulation of flow through perforated plates (Erdal and Andersson, 1997; Erdal, 1997; Frattolillo and Massarotti, 2002) some issues related to turbulence models, near wall treatment and refinement of the mesh have not yet been properly explained.

2. DESCRIPTION OF EXPERIMENTAL FACILITY AND MEASUREMENTS

A schematic of the facility used in the experiments is shown in Fig 2. Water, at room temperature, is pumped from a storage tank through an orifice plate flow meter and into the test section. Assembled in the flange of the inlet of the test section there is a perforated plate flow conditioner with the purpose to decrease flow perturbation caused by pipe bends upstream of the section. The mass flow of the experiments was set to 3.32 kg/s. The orifice plate flow meter followed the recommendations of the ISO standard 5167. The temperature of the tests was measured with a type K thermocouple located at the inlet of the test section. The tests were performed at room temperature.

The test section is a square duct made of clear acrylic with internal side of 72.14 mm and a total length of 3435.9 mm. The section is divided in two halves with flanges on both ends. The perforated plates, also made of acrylic, were positioned in the middle of the section by means of a holding flange.

Sixteen pressure taps were drilled along one wall of the test section. The upper and lower taps, located in the undisturbed region of the flow (see Fig 2), were used to measure the pressure loss coefficient. Fourteen taps, located very close to each other right downstream of the plate, were used to raise the recovering pressure profile. In order to keep them as close as possible, a special device was built for the connections with the transducers. Figure 3 shows photos of the connection device. The absolute pressure was taken on the opposite wall near the plate.

The perforated plates tested were 20 mm thick and had 25 identical holes in a square arrangement with a pitch of 14.3 mm. Two distinct hole diameters were chosen so as to cover the range of free flow area coefficients (free flow area/channel area), f, most commonly found in bottom pieces of PWRs. Plates with straight and chamfered orifice inlets were tested. Table 1 lists the geometrical features of the plates tested. In Fig. 2 there is a photo of a plate already assembled in the holding flange.

The signals from the transducers were sent to a data processing station which converted them in engineering data, performed the error analysis and stored them.

3. NUMERICAL METHODOLOGY

The simulations were performed with the commercial CFD code, CFX 10.0 (CFX, 2006). In order to check if the flow was fully developed in the test section, a simulation of the region upstream the section was performed first. The results showed that, even with the conditioner, the flow presented some asymmetry at the inlet of the section. A simulation with plate number 1 was then performed using the results of the previous calculations as the inlet boundary conditions. Another simulation was performed using a 1/8 symmetry and adopting a uniform velocity profile as the inlet boundary condition. The results showed negligible differences. Therefore, it was decided to perform all the calculations with the 1/8 symmetry, for it drastically reduces computing time.
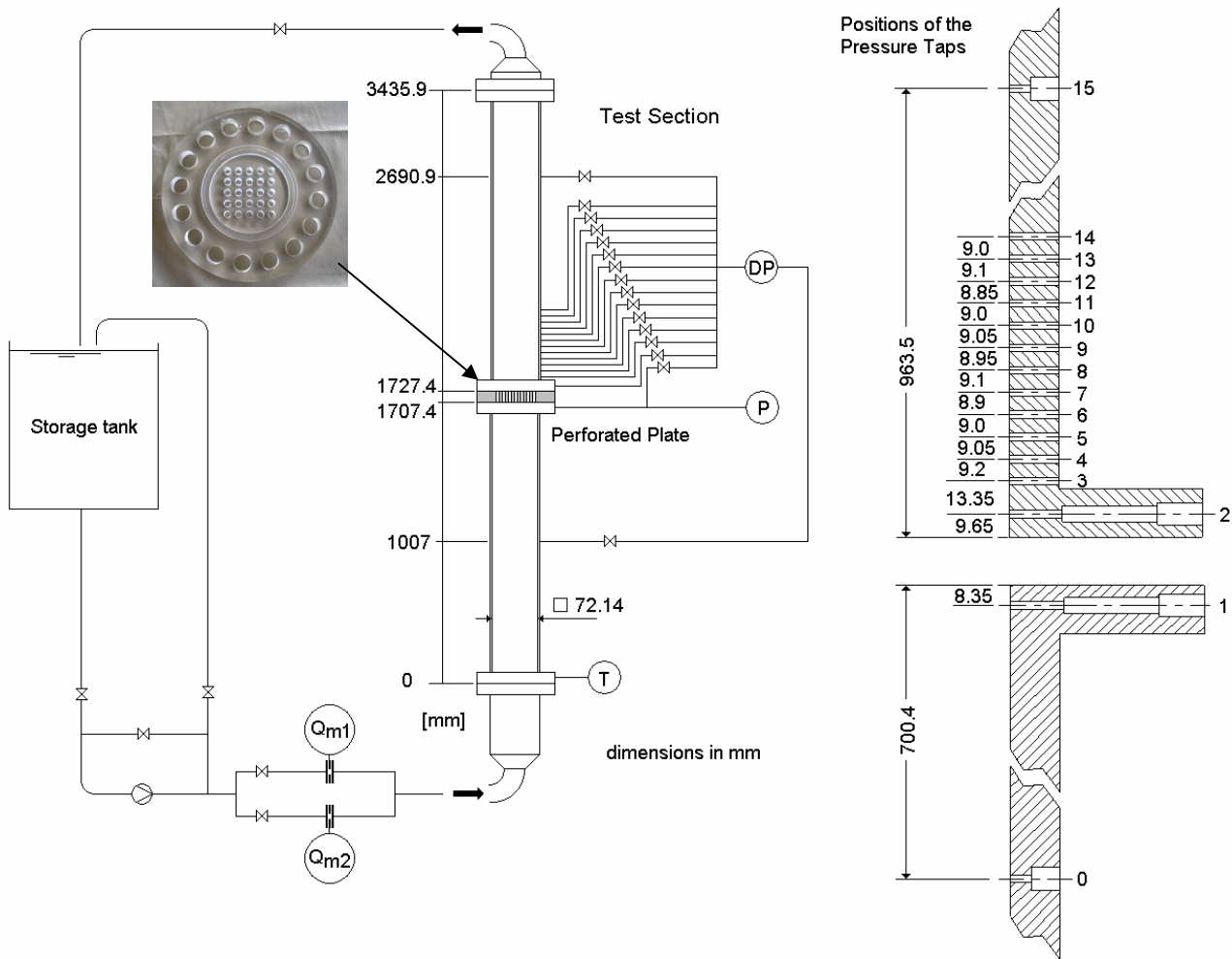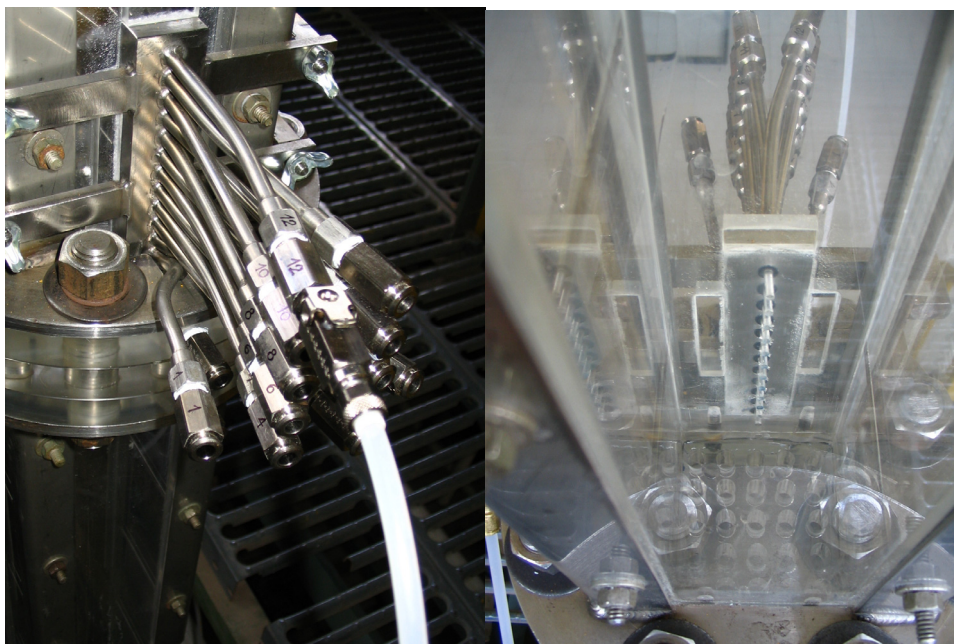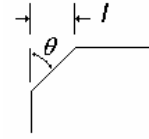
Figure 2. Schematic of experimental facility.

Figure 3. Pressure connection device

Table 1. Dimensions of the plates

Plate number	Pitch [mm]	Width [mm]	Orifice diameter [mm]	f	Characteristics of the chamfer	
					Dimension l – [mm]	Angle θ – [degree]
1			8.66	0.283	0	0
2			8.64	0.283	1.792	60
3	14.3	20	10.68	0.430	0	0
4			10.69	0.431	1.445	60
5			10.69	0.431	1.170	30

The level of turbulence is also requested as inlet boundary condition. Here again simulations with different degrees of turbulence at the inlet were performed to check its influence on the results, showing no relevant differences. However, because of the flow conditioner at the test section's inlet, the level of turbulence intensity was set to the maximum allowed by the code, 10%.

The mesh presented three different regions. A finer mesh was used in the region from 20 mm upstream to 30 mm downstream of the plate. The characteristic dimension of this part of the mesh was set to 0.5 mm. From 30 mm to 230 mm downstream the plate, a mesh with a characteristic dimension of 1.5 mm was used. This is supposed to cover the region of disturbed flow, where velocity and turbulence fields change abruptly. The rest of the test section was covered by a coarser mesh with a characteristic dimension of 3 mm. Those values were chosen after a mesh refinement study which showed that further refinement would drastically increase computational efforts and give no correspondent increase in the quality of the results. Figure 4 shows some details of the mesh in the central plane of the flow channel.
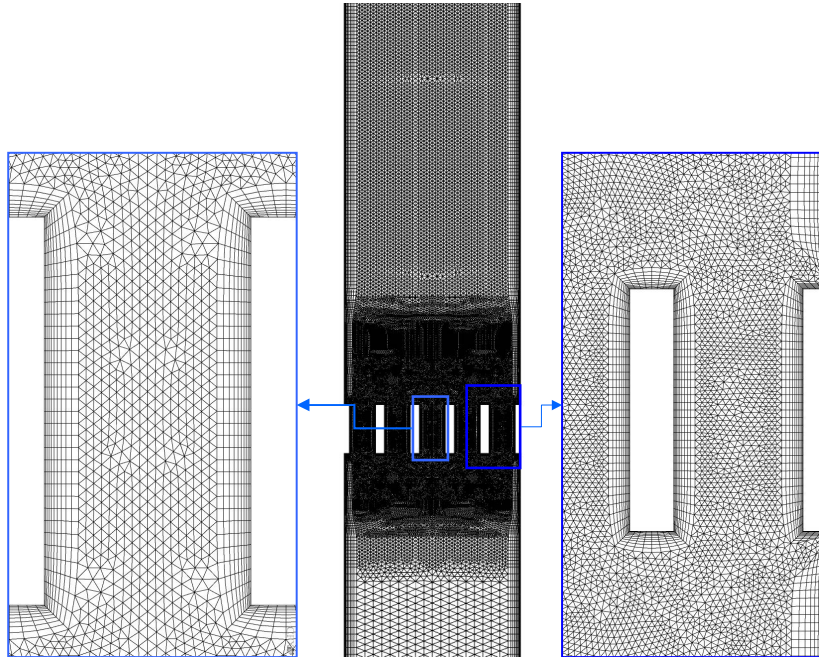

Figure 4. Details of the mesh used in the simulations.

The RANS (Reynolds Averaged Navier-Stokes) equations were solved together with an eddy viscosity turbulence model. Among the various turbulence models available in the code, the standard k-ε and the SST (Shear Stress Transport) were chosen for this work. They were adopted in this work mainly because of their numerical robustness and fast convergence.

The k-ε model, developed by Launder and Spalding (1974), assumes that the turbulence viscosity is related to the turbulence kinetic energy and dissipation. In CFX the k-ε model uses a scalable wall-function approach to improve the near wall treatment which is made with the log-law function. The basic idea behind the scalable wall function is to limit a lower value for the dimensionless distance from the wall (y^+) in the log-law region in such a way that all the mesh points are outside the viscous sub layer. In this way all fine mesh inconsistencies near the wall can be avoided.

In the Shear Stress Transport (SST) model, formulated by Menter (1994), the turbulent viscosity is modified to account for the transport of the turbulent shear stress. The model uses a function to blend an accurate near the wall model and the k-ε formulation in the outer region. This wall function uses two equations, a linear equation for the viscous sub-layer and a log-law equation outside. Both equations are weighed in a manner that, if the first node of the mesh is within the viscous sub-layer the velocity is defined more by the linear equation, if it is out, the velocity is defined more by the log-law.

The numerical schemes applied for the simulations were second-order central difference scheme for the diffusion terms and a high resolution (formally second-order) upwind scheme for the convective terms. The high resolution scheme developed by Barth and Jesperson (1989) reduces numerical diffusion and dispersion by evaluating the scheme locally applying the highest order possible, between first and second-order, that does not violate the boundedness principles.

Near the walls, layers of extruded mesh were used to capture the effects of the boundary layer in all simulations (Fig. 4). An effort was made to keep the value of the first dimensionless wall parameter (y^+) less than 10. This doesn't make much difference for the k-ε model and allows for the SST model take advantage of the automatic near wall treatment of the code.

4. RESULTS

The experimental results are summarized in Tab. 2. The evaluated uncertainties for the measured parameters are: mass flow (q_m): 0.023 kg/s; absolute pressure (P): 0.02 bar ; test temperature (T): 1 ^oC ; Reynolds number (Re): 1533 and differential pressure (DP): 0.1 mbar

Table 2. Experimental results

Plate		1	2	3	4	5
Test conditions	q_m [kg/s]	3.318	3.324	3.322	3.317	3.321
	P [bar]	0.880	0.695	0.690	0.686	0.691
	T [^oC]	31.9	33.4	28.7	28.8	30.9
	Re	60376	62365	56411	56493	59166
Tap pressure drops [mbar]	0-1	0.62	0.47	0.56	0.48	0.48
	0-2	30.95	29.66	12.64	11.17	10.88
	0-3	26.88	25.57	8.80	7.52	7.09
	0-4	23.79	22.30	7.93	6.48	6.06
	0-5	21.97	20.30	7.50	6.20	5.62
	0-6	20.76	18.91	7.23	6.02	5.51
	0-7	20.17	18.46	7.08	5.91	5.41
	0-8	20.07	18.20	7.01	5.80	5.37
	0-9	19.96	18.32	7.00	5.88	5.32
	0-10	19.94	18.46	6.89	5.87	5.48
	0-11	19.91	18.12	7.00	6.03	5.31
	0-12	19.96	18.13	6.97	6.02	5.45
	0-13	20.03	18.14	7.09	5.96	5.40
	0-14	19.96	18.13	7.09	5.98	5.41
	0-15	20.30	18.64	7.39	6.35	5.74

A comparison between experimental and calculated results is shown in Tab. 3. The values of *DP* listed here were taken from pressure taps 0 and 15, in the undisturbed flow regions.

As can be easily noticed from Tab. 3, with the exception of plate 5, there is a large discrepancy between experimental and numerical results. Although the standard k-ε turbulence model can be very precise for water flows in simple geometries like circular sections with sudden obstructions and expansions of the flow (Burden and McLaury , 2002; Barros Filho, 2006), in more complex geometries, it is known to give poor results (Tzanos, 2001). The data here seem to confirm it. An examination of Tab. 3 indicates that, the more disturbed the flow, the worse is the result. The simulations of the plates with sharp orifice inlets gave discrepancies greater than two times those with chamfered inlets,

for the same orifice diameter. Also, comparing only the plates with sharp orifice inlets, plate number 1, with a smaller *f*, has a greater discrepancy than plate number 3.

Table 3. Comparison between experimental and calculated data

Plate	DP experimental [mbar]	DP calculated [mbar]			
		k-ε	Diff %	SST	Diff %
1	20.30	26.12	28.66	26.21	29.11
2	18.64	20.93	12.29	20.52	10.09
3	7.39	8.98	21.52	9.00	21.79
4	6.35	6.99	10.08	6.98	9.92
5	5.74	5.77	0.52	5.65	-1.60

It is surprising that both turbulence models used gave so close results. The SST model is supposed to be more accurate, for it accounts more appropriately for the near the wall velocity field than the standard *k-ε* model. Figure 5 shows a contour plot of the axial velocity in the central plane of the section, calculated with the two turbulence models. It can be seen that the SST model represents more accurately the recirculation zones that are expected to appear at the inlet and downstream of the orifice outlet.
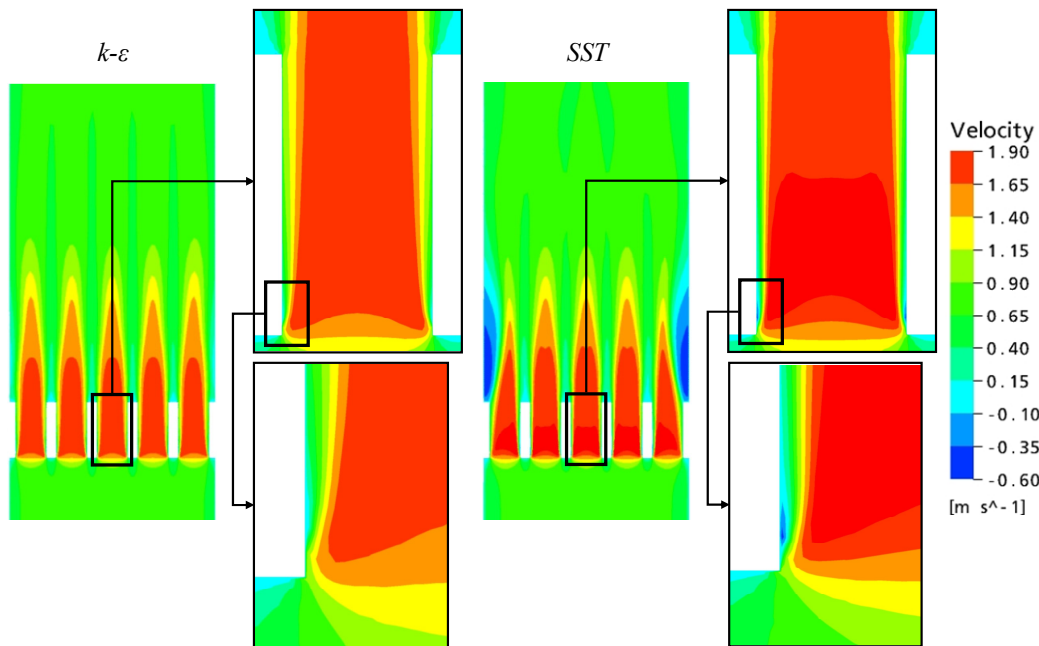

Figure 5. Plot of the axial velocity contours in the central plane of the test section.

Table 4 shows a comparison of the pressure loss coefficient *K* obtained in this work with the values calculated with the Idelchik Handbook (Idelchik, 1960). This coefficient is given by the formula:

$$DP = (K \rho v^2)/2 \tag{1}$$

Where ρ is the density and v the velocity in the flow channel.

The values of *DP* used in the calculation of *K* were also taken from taps 0 and 15. The comparison refers only to the plates with sharp orifice inlets because the Handbook doesn't account properly for chamfered inlets. The old version of the Idelchik Handbook was used here because it is more adequate for the Reynolds numbers of the tests. Although this Handbook is widely used in pressure loss calculations, even in the nuclear industry, it can not be considered accurate for the plates tested here (IAEA, 2001). Even so, it gave results much closer to the experiments than the simulations.

Table 4. Comparison between experimental and calculated pressure loss coefficient.

Plate	K experimental	K calculated					
		k-ε	Diff %	SST	Diff %	Idelchik	Diff %
1	9.36	12.22	30.56	12.26	30.98	10.44	11.53
3	3.00	3.78	26.00	3.78	26.00	3.16	5.33

Figure 6 shows plots comparing the calculated and experimental pressure recovery downstream of the plates. The plots cover a portion of the test section from 20 mm upstream to 140 mm downstream the plate. The experimental points refer to the pressure taps 1 to 14 (see Fig. 1). In the figure, two vertical lines show the position of the plate.

Here again the calculated values differ significantly from the experimental (with the exception of plate 5). Once again the curves show no noticeable differences in the values calculated with the two different turbulence models used in the simulations. They differ only inside the orifices. This is still more unexpected than in the case of the total loss (Tab. 3), once, as can be seen from Fig 4, the recovering region presents rather different patterns of flow in the two simulations.
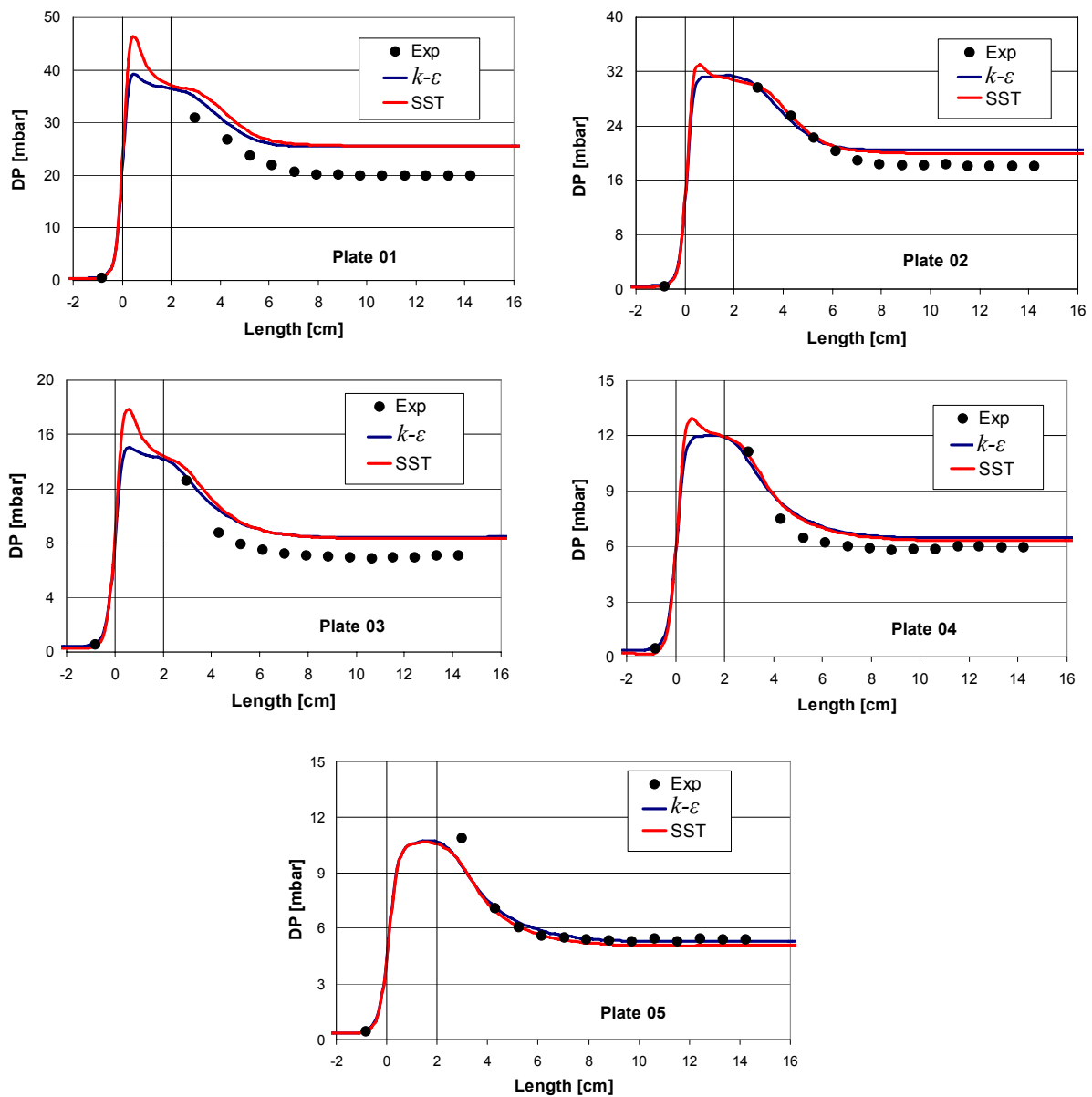

Figure 6. Calculated and experimental pressure recovery.

5. CONCLUSION

Experimental tests were performed where the pressure loss of water flow through perforated plates were measured. The results were compared with simulations performed with the commercial code CFX. The simulations were done with two different turbulence models, the standard k-ε and the SST. Both gave very close results but with great discrepancies to the experiment. It is important to stress here that those models were chosen among others more "advanced" available in the code, because of their numerical robustness, fast convergence and straightforward use. These features are expected in a calculation intended for licensing purposes in the nuclear industry.

There seems to be a direct correspondence between the degree of disturbance of the flow and the discrepancy in the results. This fact seem to confirm other works reporting the inadequacy of the standard k-ε model for flows in complex geometries with sudden area change.

The SST model, however, was expected to give better results. Once the disturbance of the flow in the tests here seems to be caused mainly by the plate face upstream the flow, it can be that an even more refined mesh in that region may yield better results. In the mesh refinement study performed, the regions just up and downstream the plate were set to the same mesh dimension.

In the sequence of the work initiated here, different types of perforated plates and other turbulence models will be tested.

6 AKNOWLEDGMENTS

6. REFERENCES

Anglart, H., et alli, 1997, "CFD prediction of flow and phase distribution in fuel assemblies with spacers", Nuclear Engineering and Design, Vol. 177, pp. 215–228

Aszodi, A.; Legrad, G., 2002, "Detailed CFD analysis of coolant mixing in VVER-440 fuel assemblies with the code CFX-5.5", Technical Meeting on Use of Computational Fluid Dynamics (CFD) Codes for Safety Analysis of Reactor Systems, including Containment, Pisa, Italy.

Barros Filho, J. A., 2006, "Comparação entre simulações bi e tridimensionais com o CFX", Internal Report, NI – EC3-15/06, CDTN/CNEN, Belo Horizonte.

Barth, T. J. and Jesperson, D. C., 1989, "The design and application of Upwind schemes on unstructured meshes" American Institute of Aeronautics and Astronautics Journal, Paper 89-0366.

Burden, T. L., McLaury, B. S., 2002, "Laser Doppler velocimeter measurements to characterize turbulence in a constriction with sharp and rounded inlets", Experiments in Fluids, Vol. 32, pp. 472–480.

CFX-10.0, 2006, "User manual", ANSYS-CFX.

Erdal, A., Andersson, H. J., 1997, "Numerical aspects of flow computation through orifices", Flow. Meas. Instrum, Vol 5, pp. 27-37.

Erdal, A., 1997, "A numerical investigation of different parameters that affect the performance of a flow conditioner", Flow. Meas. Instrum, Vol. 8, pp. 93-102.

Frattolillo, A. and Massarotti, N., 2002, "Flow conditioners efficiency a comparison based on numerical approach", Flow Meas. Instrum, Vol.13, pp. 1-11.

Gan, G. and Riffat, S. B.,1997, "Pressure loss characteristics of orifice and perforated plates", Experimental Thermal and Fluid Science, Vol. 14, pp 160-165.

Hoehne, T. , et alli, 2000, "Numerical investigation of the coolant mixing during fast deboration transients in Konvoi type reactors", CFX Users Conference, Unterhaching / Germany

IAEA , 2001, "Thermohydraulics Relationships for Advanced Water Cooled Reactors", TECDOC-1203.

Idelchik, I. E., 1960, "Handbook of hydraulic resistance", third edition, CRC Press Inc., Boca Raton.

IAEA, 2002, "Use of computational fluid dynamics codes for safety analysis of nuclear reactor systems", TECDOC-1379.

Jeon, J. H., Han, B. S., 2005, "A CFD analysis of coolant flow in a PWR lower plenum without geometrical simplification (Draft)", ICONE13-50621 - 13th International Conference on Nuclear Engineering, Beijing, China.

Launder, B. E. and Spalding, D. B., 1974, "The numerical computation of turbulent flow", Computer Methods in Applied Mechanics and Energy, Vol. 3, pp. 269-289.

Liu, B.; et alli, 2005, "CFD approach for investigating flow and heat transfer in PWR fuel assembly", ICONE13-50924 - 13th International Conference on Nuclear Engineering, Beijing, China.

Menter, F. R., 1994, "Two-equation eddy-viscosity turbulence models for engineering applications", AIAA-Journal, Vol. 32, pp. 269-289.

Sahin, B. and Ward-Smith, A. J., 1987, "The use of perforated plates to control the flow emerging from a wide-angle diffuser with application to electrostatic precipitator design", J. Heat Fluid Flow, Vol. 8, pp. 124-131.

Schlüter, Th. and Merzkirch, W., 1996, "PIV measurements of the time-averaged flow velocity downstream of flow conditioners in a pipeline", Flow Meas. Instrum., Vol. 7, pp. 173-179.

Spearman, E. P., Sattary, J. A. and Reader-Harris, M. J., 1996, "Comparison of velocity and turbulence profiles downstream of perforated plate flow conditioners", Flow Meas. Instrum., Vol. 7, pp. 181-199.

Tzanos, C. P.,2001, "Performance of k-ε Turbulence Model in the Simulation of LWR Fuel Bundle Flow", Trans. Am. Nucl. Soc., Vol. 84, pp. 197-203 .

Yadigaroglu, G.. Andreani, M.. Dreier. J., Coddington. P., 2003, "Trends and needs in experimentation and numerical simulation for LWR" safety", Nuclear Engineering and Design., Vol. 221, pp. 205–223.

5. RESPONSIBILITY NOTICE

The authors are the only responsible for the printed material included in this paper.